Theoretical calculation of the optical-phonon deformation potentials on the Lambda axis in the Brillouin zone for tetrahedral semiconductors

1992 J. Phys.: Condens. Matter 4 6735

(http://iopscience.iop.org/0953-8984/4/32/008)

J. Phys.: Condens. Matter 4 (1992) 6735–6742. Printed in the UK

Theoretical calculation of the optical-phonon deformation potentials on the Λ axis in the Brillouin zone for tetrahedral semiconductors

Ren-Zhi Wang†, San-Huang Ke† and Mei-Chun Huang‡

† Department of Physics, Xiamen University, Xiamen 361005, People's Republic of China
‡ Centre of Theoretical Physics, Chinese Centre of Advanced Science and Technology (*World Laboratory*), *Beijing, People's Republic of China*

Received 28 January 1992, in final form 23 April 1992

Abstract. In this paper, the *ab initio* calculations of optical-phonon deformation potentials (ODPs) d_{30}, $d_{10}(\mathrm{val})$ and $d_{10}(\mathrm{con})$ on the Λ axis in the Brillouin zone for 12 elemental and compound semiconductors are reported. This work is based upon the density-functional theory LMTO ASA band-structure method with a frozen-phonon model. The ODP values as functions of the k-points and their material dependences have been investigated.

1. Introduction

In the study of resonant Raman scattering of tetrahedral semiconductors, the optical-phonon deformation potentials (ODPs) are important parameters which describe the interaction between electrons and long-wavelength optical phonons. Recently, the main theoretical work pertaining to these parameters includes calculations using the non-local empirical pseudopotential method (NEPM) by Pötz and Vogl [1] and the empirical tight-binding calculations by Blacha *et al* [2] as well as several first-principles studies including first-principles tight-binding, linear-muffin-tin-orbital (LMTO) and *ab initio* pseudopotential calculations (namely the first-principles pseudopotential method (FPPM)) by Christensen *et al* [3], Brey *et al* [4], Nielsen and Martin [5], Wang *et al* [6] and Gu *et al* [7]. The tight-binding method [4, 5] gave only the d_0-value at the Γ point. If the differences of strain pattern adopted to simulate the role of optical phonons in theoretical calculations of ODPs are considered, one can find two strain models in the recent literature. The first model is the rhombohedral strain model as used in [4, 5]. The practical way to achieve this is as follows: introduce a rhombohedral strain (i.e. a trigonal deformation with a [111] direction as the strain axis) to produce a splitting of $E_v(\Gamma)$ and carry out the trigonal shear deformation potential d; then, use the relation $d = d' - \frac{1}{4}\xi d_0$ including an internal-strain parameter ξ to determine the ODP d_0. This model can calculate only d_0 of the ODPs. The second model is the frozen-phonon model as used in [1, 6, 8, 9, 10], in which a displacement of the two sublattices without changing the translation vector (i.e. an optical phonon at $k = 0$) is introduced to split and shift E_v and E_c. Then, the ODPs d_0, d_{30}, $d_{10}(\mathrm{val})$ and $d_{10}(\mathrm{con})$ at the Γ or L point are found in terms of the relations between the eigenvalue changes and the displacement of the two sublattices. The application

0953-8984/92/326735+08$04.50

of this model to GaAs, AlAs, GaP and $Ga_{1-x}Al_xAs$ [8, 9] shows that it has good accuracy and can be applied directly to calculate the d_{30}, $d_{10}(\mathrm{val})$ and $d_{10}(\mathrm{con})$ on the Λ axis. The ODPs included in the Raman tensor of the E_1 gap are those on the Λ axis. For this reason, Renucci *et al* [11] and Renucci *et al* [12] investigated the ODP values on the Λ axis with the empirical pseudopotential method and kp perturbation for the study of resonant Raman scattering in Ge and Si. As to the *ab initio* calculation, which is expected to be more complicated than the empirical method in the theoretical sense, only the results at the Γ and L points were reported. Few investigations for the Λ axis have been found in the recent literature. As the rhombohedral strain model can give only the d_0-value, in this paper we adopted the frozen-phonon model mentioned above for the LMTO band-structure method in the atomic-sphere approximation (ASA) to calculate the ODPs on the Λ axis for 12 tetrahedral semiconductors.

2. Method and results

When the LMTO ASA method is applied to open-structure tetrahedral semiconductors, it is necessary to introduce 'empty spheres'. The positions of atoms A and B and the empty spheres E_A and E_B in a primitive cell are (000), $(111)\alpha/4$, $(111)\alpha/2$ and $(111)3\alpha/4$ respectively. E_A (E_B) is located at the centre of the tetrahedron constructed by the atomic sphere A (B). In tetrahedral semiconductors, the long-wavelength optical phonon has Γ_{15} symmetry which presents a relative vibration between the two sublattices along the [111] direction without changing the translation vector [1, 2]. The ODP d_0 is determined by the splitting of the $E_v(\Gamma)$ state produced by the Γ_{15} phonon. Similarly, the ODPs d_{30}, $d_{10}(\mathrm{val})$ and $d_{10}(\mathrm{con})$ are determined by the splitting and shift of the $E(\mathrm{L})$ states induced by the Γ_{15} phonon displacement which is decomposed into the $L_1 + L_3$ representation of the k-group C_{3v} at the L point [1, 6]. In this paper, we use the relative displacement between atoms A and B, similarly to the NEPM calculation within the frozen-phonon model [1], to simulate the Γ_{15} optical-phonon mode. The difference from the NEPM is that, in the LMTO ASA method, the displacement partners for empty spheres are also needed for a proper treatment of the situation. On the basis of the adiabatic approximation, we have suggested a frozen-phonon approximation in which the empty spheres are considered to match their atomic-sphere partners. In other words, we use the relative displacement between the A atom tetrahedron together with empty sphere E_A and the B atom tetrahedron together with empty sphere E_B to simulate the role of the Γ_{15} vibration mode [8–10]. Throughout this paper, this theoretical model is used.

After obtaining the valence band splitting ΔE_v, valence band shift δE_v and conduction band shift δE by self-consistent band-structure calculations in the two cases of $u_r = 0$ and $u_r \neq 0$, we use the following relations which have been used in the NEPM [1] to give the d_{30}-, $d_{10}(\mathrm{val})$- and $d_{10}(\mathrm{con})$-values at the L point:

$$\delta E(\mathrm{L},\mathrm{val}) = [(e_v \cdot u_r)/2\alpha]d_{10}(\mathrm{val}) \tag{1}$$

$$\delta E(\mathrm{L},\mathrm{con}) = [(e_v \cdot u_r)/2\alpha]d_{10}(\mathrm{con}) \tag{2}$$

$$\Delta E(\mathrm{L},\mathrm{val}) = (|e_v \times u_r|/\alpha)d_{30}. \tag{3}$$

For the Γ point, the d_0-value is given by

$$\Delta E(\Gamma_{15v}) = \tfrac{3}{2}(|u_r|/\alpha)d_0 \tag{4}$$

in which the spin–orbit coupling term has been neglected. Here, α is the lattice constant, e_v is the unit vector for the energy valley position vector and $u_r = (\delta\delta\delta)\alpha/4$. It should be noted that the symmetry of the Λ axis is the same as the L point (C_{3v} symmetry). So, the formulae for the L point can be used directly for the Λ axis only with the L replaced by Λ in the left-hand side of equations (1)–(3). It can be seen that the above relations for the Λ axis are consistent with those used by Renucci *et al* [11] only with different presentation forms. Specifically, the $\delta E(\Lambda, \mathrm{val})$, $\delta E(\Lambda, \mathrm{con})$ and $\Delta E(\Lambda, \mathrm{val})$ in this paper correspond simply to the energy shift $\langle\psi_3^v|V|\psi_3^v\rangle_{111}$, $\langle\psi_1^c|V|\psi_1^c\rangle_{111}$ and the energy splitting value Δ, respectively, in [11].

Because of the computational effort and accuracy, we choose evenly 11 k-points on the whole Λ axis and determine the ODP values for each k-point and then line up these data points smoothly to show the variations in ODP values with k. The shallow d electrons of atoms Ga and Zn are treated as valence electrons in the LMTO ASA (scalar relativistic) band calculation. The δ-value in the relation $u_r = (\delta\delta\delta)\alpha/4$ is set in the range $-0.002 \leqslant \delta \leqslant 0.002$. The calculated results are illustrated in figure 1 and figure 2. Table 1 gives the results at the Γ and L points. The results from the NEPM [1] are also listed in table 1 for comparison.

Table 1. Values of d_0 (at the Γ point) and d_{30}, $d_{10}(\mathrm{val})$ and $d_{10}(\mathrm{con})$ (at the L point) given by the present work and the NEPM [1].

	d_0		d_{30}		$d_{10}(\mathrm{val})$		$d_{10}(\mathrm{con})$	
	This work	NEPM	This work	NEPM	This work	NEPM	This work	NEPM
Si	40.2	37.9	49.0	44.8	−20.8	−16.4	−3.7	−10.4
Ge	39.3	37.0	47.0	48.3	−13.6	−10.2	−24.9	−27.7
Sn	31.6	30.3	38.1	37.6	−9.5	−7.3	−22.4	−17.7
AlSb	26.7		35.6		−15.7		−15.5	
AlAs	24.6		35.0		−18.2		−12.0	
AlP	23.7		33.9		−18.2		−4.4	
GaSb	32.9	29.3	41.1	38.7	−9.2	−11.9	−24.7	−30.6
GaAs	29.6	29.1	41.6	40.3	−10.2	−11.1	−26.1	−21.7
GaP	28.3	26.5	41.3	38.5	−10.2	−11.4	−20.8	−17.7
ZnTe	16.4		27.9		−5.1		−21.5	
ZnSe	11.7	21.6	24.9	28.9	−2.1	−14.2	−23.8	−8.9
ZnS	8.5		22.1		+1.4		−22.4	

3. Discussion

3.1. Comparison between the present results and those of the NEPM [1] and the FPPM [6]

Of the various band-structure methods, the band structure resulting from the NEPM is in the best agreement with the experimental results. In fact, the ODP values from the NEPM in [1] are also the most comprehensive theoretical results at the Γ and L points. In table 1, one can see that, except for d_0, $d_{10}(\mathrm{val})$, $d_{10}(\mathrm{con})$ for ZnSe and $d_{10}(\mathrm{con})$ for Si, the two sets of results are fairly close to each other. For ZnSe, in

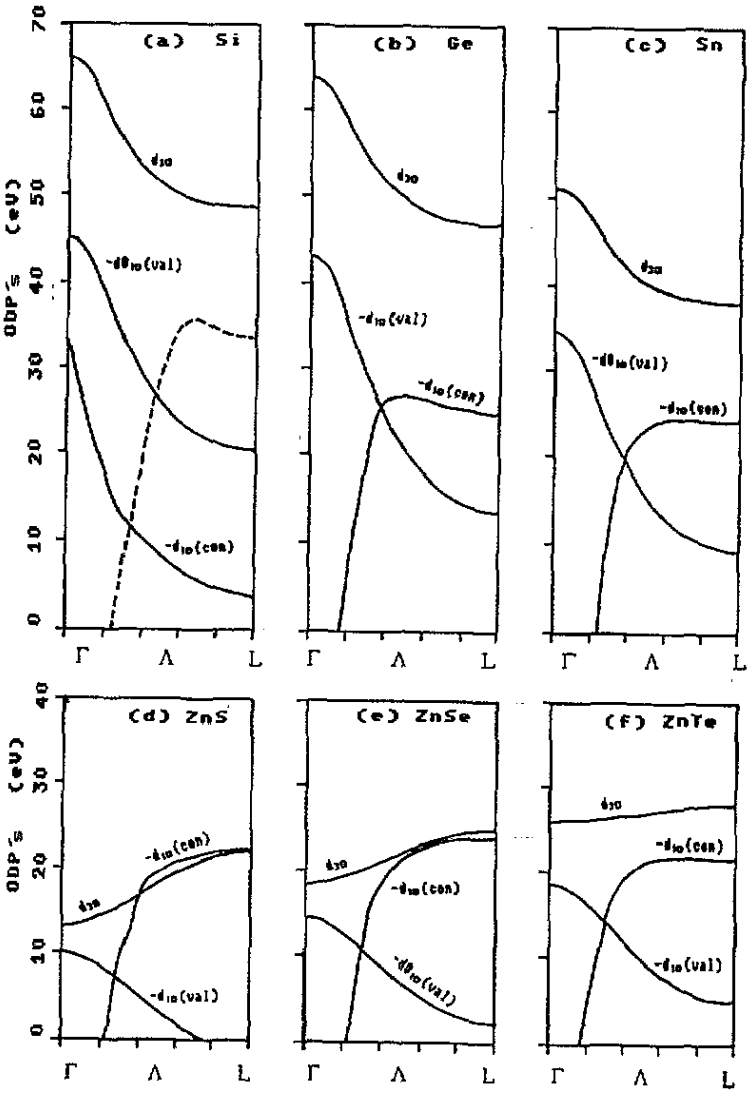

Figure 1. The variations in d_{30}, d_{10}(val) and d_{10}(con) for the elemental crystals Si, Ge and Sn and the group II–VI compounds ZnS, ZnSe and ZnTe with k along the Λ axis.

this paper we treat the Zn 3d electrons as valence electrons and perform the energy band calculation including the d band on the assumption that the Zn 3d level has already entered the energy range of the valence band formed by the 4s and 4p states. In other words, the hybridization of the d state with the energy band formed by the s and p states is included by the diagonalization processes for solving the secular equation. In contrast with this, in the NEPM calculations this d-state hybridization is taken into account by the non-local part of the pseudopotential. It is expected that these different treatments of the d state cause the difference between our results and those of the NEPM. We believe that treating the 3d electrons as valence electrons is more reasonable.

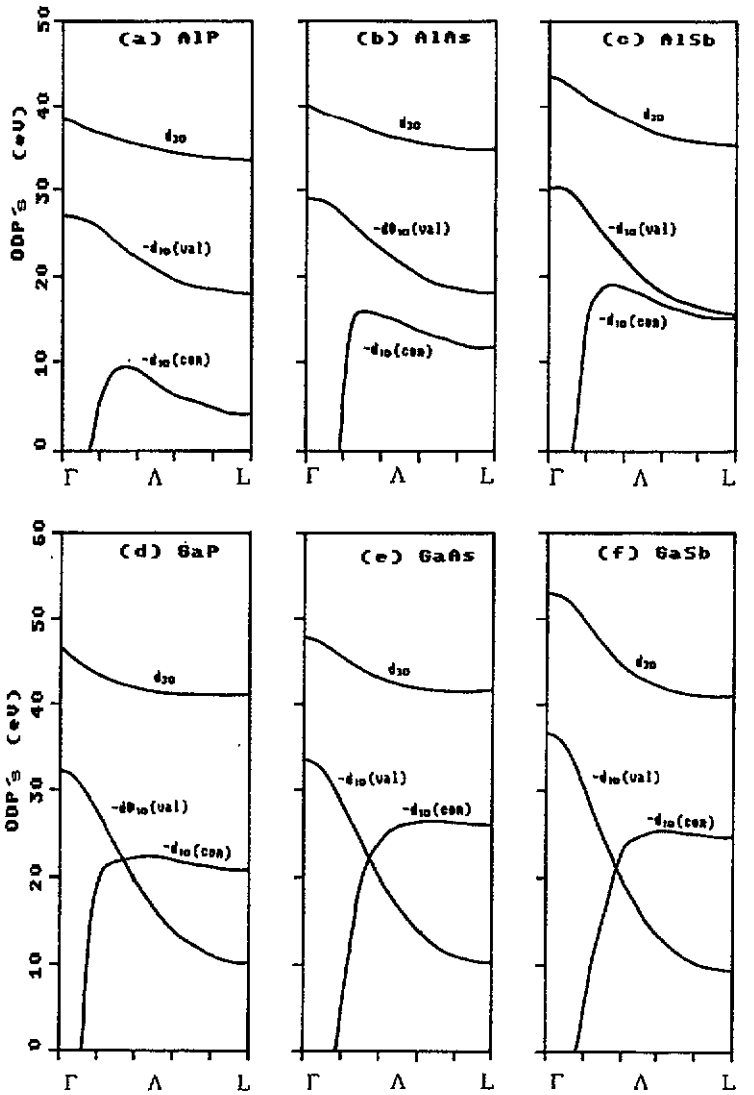

Figure 2. The variations in d_{30}, $d_{10}(\mathrm{val})$ and $d_{10}(\mathrm{con})$ for the group III–V compounds AlP, AlAs, AlSb, GaP, GaAs and GaSb with k along the Λ axis.

Recently, the FPPM has been applied to ODPs [6, 7]. In [7], only the investigation of d_0 at the Γ point was reported while, in [6], the ODPs at the L point were also determined besides d_0. The results of this work, the NEPM [1] and the FPPM [6] together with its quoted experimental values are listed in table 2. The formula used in [6] for $d_0^{\prime v}$ (non-relativistically calculated) is different from the normal definition of d_0 by a coefficient $\frac{3}{2}$ [7, 13] and, as a result, the $d_0^{\prime v}$-values are obviously larger; in table 2 we give only the relativistically calculated d_0-value (i.e. d_0^{v}) of [6]. It appears that the FPPM d_0-values are somewhat larger than those of this work and the NEPM and are closer to the experimental data. This consistency with experiments is thought to be due to including the strain-induced changes in the non-spherical potential in the calculation in [6]. In table 2 the d_{30}-, $d_{10}(\mathrm{val})$- and $d_{10}(\mathrm{con})$-values of the FPPM

are markedly larger than those of the present work and the NEPM but, for GaAs, the three values of R_d, which is defined as $R_d = |d_{30}/[d_{10}(\text{con} - d_{10}(\text{val})]|$ and can be determined experimentally, are close to each other and very consistent with the experimental value. However, in the case of GaP, the three R_d-values are relatively scattered and ours is between the NEPM result and the FPPM result. To the best of our knowledge, no experimental value is available for comparison.

Table 2. Values of d_0, d_{30}, $d_{10}(\text{val})$, $d_{10}(\text{con})$ and R_d given by this work, the NEPM [1], the FPPM [6] and experiments.

		d_0	d_{30}	$d_{10}(\text{val})$	$d_{10}(\text{con})$	R_d
GaAs	This work	29.6	41.6	−10.2	−26.1	2.62
GaAs	NEPM [1]	29.1	40.3	−11.1	−21.7	3.8
GaAs	FPPM [6]	34.0	50.13	−37.2	−54.34	2.92
GaAs	Experiment	41.48				3.0
GaP	This work	28.3	41.3	−10.2	−20.8	3.9
GaP	NEPM [1]	26.5	38.5	−11.4	−17.7	6.1
GaP	FPPM [6]	31.5	50.98	−10.0	−35.93	1.97
GaP	Experiment	44.0				

3.2. The effect of strain models on d_0-values

In table 3, both d_0^{ASA} (this work) and d_0^{NEPM} (NEPM) are obtained from the frozen-phonon model. d_0^{LMTO} is obtained from the rhombohedral strain model (determined from $d = d' - \frac{1}{4}\xi d_0$) and Δd_0 is a non-spherical correction term to d_0^{LMTO} determined by Brey *et al* [4]. The energy band method for d_0^{ASA} and d_0^{LMTO} are the same (the LMTO method), but the strain model is different. As a result, the two values are obviously different from each other. On the other hand, d_0^{ASA} and d_0^{NEPM} are given by two different band-structure methods (LMTO and NEPM), but the strain model is the same (frozen-phonon model) and they are very close to each other. This indicates that the strain model controls the d_0-value. By comparing d_0^{LMTO} and $d_0^{\text{LMTO}} + \Delta d_0$ with d_0^{expt}, one can see that the non-spherical correction for the LMTO method plays an important role in the d_0-value. In spite of this, d_0^{ASA} is still closer to the experimental data d_0^{expt} than is the corrected result, $d_0^{\text{LMTO}} + \Delta d_0$, for the majority of materials. This shows that the strain model plays the most important role in the d_0-value in the LMTO ASA method.

3.3. The variations in the ODPs with k along the Λ axis

In figure 1 and figure 2, it appears that for the 12 materials the $-d_{10}(\text{val})$-values decrease with increasing k-value. The variations in the d_{30}-values of elemental and group III–V compound semiconductors are also the same. For $-d_{10}(\text{con})$, Si is very different from the other 11 materials: for Si, $-d_{10}(\text{con})$ decreases with increasing k while, for the other materials, $-d_{10}(\text{con})$ increases with increasing k and appears as a 'flat shoulder' near the L point. With respect to the conduction band symmetry on the Λ axis, for Si it is $\Gamma_{15C} \rightarrow \Lambda_{1C}$ and p like and, for the other 11 materials, it is $\Gamma_{1C} \rightarrow \Lambda_{1C}$ (for the zincblende structure) or $\Gamma'_{2C} \rightarrow \Lambda_{1C}$ (for the diamond structure) and s like. We guess that the difference in the conduction band symmetry is the main

Table 3. The d_0 results for 12 semiconductors given by this work (d_0^{ASA}), the NEPM (d_0^{NEPM} [1]), the LMTO method (d_0^{LMTO}) and the corrected values of d_0^{LMTO} ($d_0^{LMTO} + \Delta d_0$) as well as the experimental data (d_0^{expt} [4]) and the ionicity parameters f_i [13].

	d_0^{ASA}	d_0^{NEPM}	d_0^{LMTO}	$(d_0^{LMTO} + \Delta d_0)$	d_0^{expt}	f_i
Si	40.2	37.9	20.9	(27.1)	40.27	0.00
Ge	39.3	37.0	22.4	(29.3)	34.39	0.00
Sn	31.6	30.3				0.00
AlSb	26.7		16.1	(21.3)	37	0.250
AlAs	24.6		14.9	(22.0)		0.274
AlP	23.7		14.4	(22.1)		0.307
GaSb	32.9	29.3	18.7	(23.4)	32	0.261
GaAs	29.6	29.1	16.8	(25.0)	48.41	0.310
GaP	28.3	26.5	16.2	(24.3)	44.47	0.327
ZnTe	16.4		10.3	(13.8)	23	0.609
ZnSe	11.7	21.6	17.1	(9.2)	12.27	0.630
ZnS	8.5		25.2	(3.5)	4	0.623

cause of the different behaviours of $-d_{10}(\mathrm{con})$ with k. In order to verify this point of view, we determine further the $-d_{10}(\mathrm{con})$-value for the Si second conduction band $\Lambda_{1C}(\Gamma'_{2C} \rightarrow \Lambda_{1C})$ (see the dotted curve in figure 1(*a*)). Obviously this curve is very similar in shape to those of the other 11 materials.

The Raman tensor of the E_1 gap is determined from d_{30} and $d_{10}(\mathrm{diff}) = d_{10}(\mathrm{con}) - d_{10}(\mathrm{val})$ and Raman experiments are sensitive only to R_d which is defined as $R_d = |d_{30}/d_{10}(\mathrm{diff})|$ [1]. The $d_{10}(\mathrm{diff})$- and the R_d-values depend upon the relative position of the $-d_{10}(\mathrm{val})$ curve to the $-d_{10}(\mathrm{con})$ curve. At the intersection of these two curves, $d_{10}(\mathrm{diff}) = 0$ and $R_d \rightarrow \infty$. From figures 1 and 2, it can be seen that only Si and three group III–V compounds containing Al do not have this intersection. In figure 3, we give the variations in R_d for Si, AlP and GaAs with k. Obviously, those for Si and AlP are very flat on the whole Λ axis, while those for GaAs are sharp near the intersection.

3.4. ODP values of different materials

In table 1, figure 1 and figure 2, it appears that the $d_{10}(\mathrm{con})$-values of all materials are very close to each other. The differences between d_0, d_{30} and $d_{10}(\mathrm{val})$ for different materials are relatively large, but the dependences on materials are also similar, i.e. Si has the largest values and ZnS has the smallest values. In table 3, we list the ionicity parameter f_i [14] in the last column. By comparing the d_0-value with f_i, one can see that, the larger f_i, the smaller the d_0-value. For example, in table 3, the f_i-values of elemental semiconductors are the smallest and the corresponding d_0-values are the largest. In the two sets of materials containing Al and Ga, the f_i-values decrease from P to Sb, and the d_0-values increase as f_i decreases. The group II–VI compounds have the largest f_i-values, and at the same time, also have the smallest d_0-values.

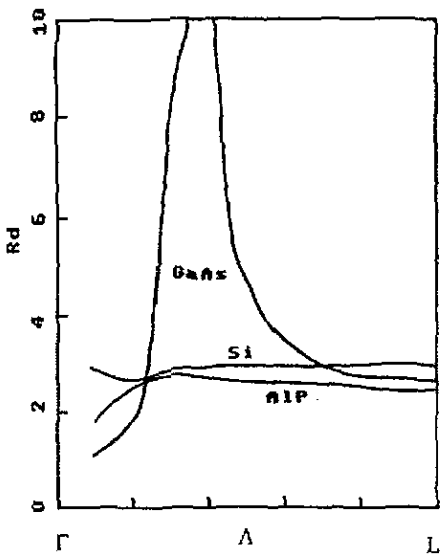

Figure 3. Curves of R_d for Si, AlP and GaAs as functions of k along the Λ axis.

Acknowledgment

This work was supported by the National Science Foundation of China.

References

[1] Pötz W and Vogl P 1981 *Phys. Rev.* B **24** 2025
[2] Blacha A, Presting H and Cardona M 1984 *Phys. Status Solidi* B **126** 11
[3] Christensen N E, Satpathy S and Pawlowska Z 1987 *Phys. Rev.* B **36** 1032
[4] Brey L, Christensen N E and Cardona M 1987 *Phys. Rev.* B **36** 2638
[5] Nielsen O H 1986 *Phys. Rev.* B **34** 5808
Nielsen O H and Martin R M 1985 *Phys. Rev.* B **32** 3780, 3792
[6] Wang B S, Gu Z Q, Wang J Q and Li M F 1989 *Phys. Rev.* B **39** 12789
[7] Gu Z Q, Li M F, Wang J Q and Wang B S 1990 *Phys. Rev.* B **41** 8333
[8] Wang R Z and Huang M C 1988 *Chinese J. Semicond.* **9** 223
[9] Wang R Z and Huang M C 1990 *Chinese Phys. (USA)* **10** 884
[10] Ke S H, Wang R Z and Huang M C 1991 *Chinese Phys. Lett.* **8** 581
[11] Renucci J B, Tyte R N and Cardona M 1975 *Phys. Rev.* B **11** 3885
[12] Renucci M A, Renucci J B, Zeyher R and Cardona M 1974 *Phys. Rev.* B **10** 4309
[13] Cardona M and Christensen N E 1990 *Phys. Rev.* B **41** 5407
[14] Phillips J C 1973 *Bonds and Bands in Semiconductors* (New York: Academic) p 43